

INTERACTION OF HYDROGEN WITH NANOPOROUS CARBON MATERIALS

T. D. Jarvi, J. Sun, L. F. Conopask, and S. Satyapal

United Technologies Research Center
Energy Systems, MS 129-90
411 Silver Lane
East Hartford CT 06108

KEYWORDS: Carbon nanotubes, carbon nanofibers, hydrogen adsorption

INTRODUCTION

High-density hydrogen storage represents a key enabling technology to the widespread implementation of portable, hydrogen-based, fuel cell systems. In the long term, portable fuel cells will use stored hydrogen fuel due to power density and systems simplification issues. Although automotive applications remain the primary industry focus at the present moment, we may expect that small portable systems will eventually become extremely important as well. Moreover, effective hydrogen storage may enable fuel cell power for a wide array of applications not presently considered viable. Clearly, fuel cell systems of any size can benefit from improved hydrogen storage technologies, therefore success in this area will have lasting societal impact.

Hydrogen's low molecular weight makes storage as a compressed gas less effective than for other fuel gases, such as methane. This fact drives compressed hydrogen storage pressures to very high values, thus requiring expensive storage systems to reach reasonable gravimetric capacities. Volumetric capacities for compressed hydrogen storage are well below the target values at pressures as high as 60 MPa. Other hydrogen storage systems have been developed including storage as a cryogenic liquid, in metal hydrides, physisorption on carbon or other sorbents, and chemical hydrides (such as dehydrogenation of organic molecules). While progress has been made, no hydrogen storage technology meets the stringent requirements that are imposed by an automotive fuel cell system [1,2].

Recently several reports have suggested that hydrogen storage in carbon nanomaterials, such as carbon nanotubes and nanofibers may exhibit storage capacity that meets (or perhaps exceeds) DOE goals for automotive fuel cell applications [1,3,4]. At first glance these suggestions appeared counter-intuitive since surface science studies of hydrogen adsorption on graphite, for example, were necessarily conducted at very low temperature in order to stabilize the adsorbate [5]. It seems clear that if the reports of high capacity are correct that these new materials must exhibit interactions with carbon that exceed those of more typical carbon materials, like activated carbon. In this study, we set out to determine if the interactions between carbon nanomaterials and hydrogen were greater than between prototypical activated carbon and hydrogen to understand these storage results.

Hydrogen storage technologies can be compared on the basis of gravimetric and volumetric storage capacities. Both of these capacities must meet certain targets in order for a hydrogen storage system to reach viability [1,2]. The storage capacity requirements for a hydrogen-fueled fuel cell vehicle derive from requiring fuel cell vehicles to exhibit comparable range and gas storage system weight and volume to conventional automobiles. To achieve a 500 km range, the hydrogen storage system must exhibit a volumetric capacity of 60 kg H₂/m³ and a gravimetric capacity of 6.2 wt. % H₂ for an installed system [1,2]. It is important to consider both gravimetric and volumetric storage capacities as weight and volume are both important in the automotive application. Another factor of prime importance is the energy penalty associated with the storage method. For example, liquifaction of hydrogen consumes about 1/3 of the lower heating value of the hydrogen. Ideal hydrogen storage systems would store hydrogen at high-density using relatively low pressure and ambient temperature.

Figure 1 compares various hydrogen storage technologies with the DOE goal [1]. Compressed gas storage is clearly the most developed technology and it shows good gravimetric capacity but low volumetric capacity at suitably high pressure. In contrast, metal hydrides show moderately good volumetric capacity, and poor gravimetric capacity. Some metal hydrides exhibit better capacities than the range indicated on Fig. 1, e.g. magnesium hydride. Generally, however, these materials suffer other problems; in the case of magnesium hydride, the dissociation temperature is very high and the material undergoes decrepitation following cycling. Newer (or perhaps resurgent) technologies for the storage of hydrogen include chemical hydrides and cryogenic adsorption on activated carbon.

Carbon nanofibers have been reported to store from 30-300% hydrogen by weight at about 112 atm [3,4]. By comparison, methane, the most compact organic arrangement of carbon and hydrogen, is 25% hydrogen by weight [6]. Despite the counter-intuitive nature of these results, because of the potential societal impact of high-density hydrogen storage, attempts were made to reproduce these results. To the best of our knowledge, other such attempts have failed [7,8].

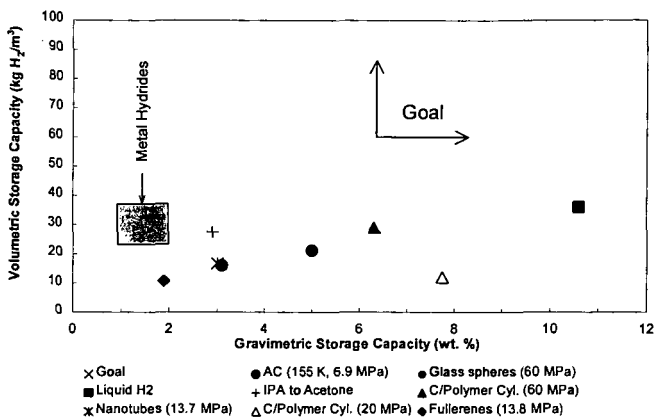


Figure 1: Comparison of gravimetric and volumetric storage capacity of various hydrogen storage technologies [1].

Recent careful studies reported that carbon nanotubes stored hydrogen at 5-10 wt% [1,9]. These later reports suggested to us that increased interactions with hydrogen arise in carbon nanotubes. Enhanced interactions were clearly required to explain the data, because typical carbon materials (activated carbon) show very low capacity at near-ambient temperature [10]. While less dramatic than the nanofiber claims, these results were very significant, in the context of Fig. 1. Especially important in these later experiments was the fact that high pressure was not required in order to store hydrogen at high density.

In general, the experimental procedures followed in the study of hydrogen storage within carbon nanomaterials have been inconsistent. This makes a systematic comparison of the various experiments impossible to perform. Nevertheless, it is useful to tabulate the results of some of these experiments. Table 1 summarizes some of the data reported in the literature for hydrogen storage in new carbon structures. Notice that the data cover a range of storage conditions and show highly variable capacity. The variety of conditions encountered in the data in Table 1 precludes a separation of the effects of storage condition from material structure (e.g. nanotube vs. nanofiber). Therefore the purpose of this study was to perform well-controlled adsorption of hydrogen on various carbon nanostructures to determine the relative interaction of hydrogen with these materials.

Sample	T / K	P / atm	$x_{wt} / \%$	Ref.
Nanofibers	298	112	35	3,4
Nanotubes	~133	~1	5-10	1,9
Nanotubes	340	136	4	11
Fullerenes	673	101	2.4	12

EXPERIMENTAL

We used the following carbon materials in this study: single walled carbon nanotubes from Rice University [13] and the University of Kentucky [14], activated carbon (BPL from Calgon Carbon Corporation), and carbon nanofibers synthesized in our laboratory. Single-walled carbon nanotubes from Rice University were estimated to be 90% pure with a diameter of 1.2 nm [13,15]. Nanotubes from the University of Kentucky were estimated as 50-70% pure SWNT by volume [14]. Carbon nanotubes were formed into "nanopipes" by processing the Rice University nanotubes [16]. A sample was placed in a mixture of concentrated sulfuric and nitric acids (3:1 by volume) and the solution was sonicated for about 24 hours at 30-40 °C. This procedure had a yield of about 50%. We synthesized carbon nanofibers by catalytic decomposition of ethylene over various catalysts in the temperature range of 500-700 °C [17]. Scanning electron microscopy and transmission electron microscopy were used to characterize the synthetic nanofibers. Calorimetry experiments made use of an isothermal flow

microcalorimeter (CSC, model 4400) at atmospheric pressure and 25 °C. Hydrogen was delivered as a pure gas at a flow rate of 10 cc/min. Degassing samples above 100 °C under vacuum overnight minimized surface contamination by residual water.

RESULTS AND DISCUSSION

Among structural questions, the nature of the synthetic nanofibers was of the greatest interest. Other researchers have characterized carbon nanotubes extensively by SEM, TEM, XRD, and Raman spectroscopy, so we did not further characterize those samples. The synthetic nanofiber sample that we were most interested in was synthesized on ceramic pellets. Insulating ceramic pellets were placed in the entrance region of the reactor in an attempt to improve the uniformity of the reactant temperature distribution. These insulating pellets were estimated to reach a temperature of ca. 500 °C during reactor operation and over several syntheses produced a large quantity of nanofiber (ca. ¼ kg) material. All of our nanofibers were synthesized using smooth surfaces.

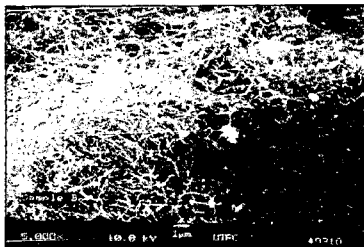


Figure 2: SEM image of carbon nanofibers synthesized by ethylene decomposition over a mixed oxide surface at ca. 500 °C.

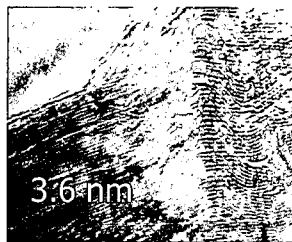


Figure 3: High resolution TEM image of carbon nanofibers synthesized by ethylene decomposition over a mixed oxide surface at ca. 500 °C.

Figure 2 shows a SEM micrograph of nanofibers synthesized on the oxide surface. In general, the structure is fibrous and few large clumps of amorphous carbon were observed in this sample. The question of the microstructure of the material could only be answered by high-resolution TEM imaging. One question was whether the structure of this material was similar to the material that Rodriguez et. al. have claimed store large quantities of hydrogen [3,4]. Figure 3 shows a high resolution TEM image of a carbon fiber synthesized on the oxide pellets. Graphite-like plane spacing is observed in this sample (ca. 0.36 nm). This measurement cannot be made to a high degree of precision without a standard specimen installed in the TEM during imaging. Therefore, this value is indistinguishable from that of graphite (0.34 nm). The plane spacing runs parallel to the fiber axis along most of its length, Fig. 3. There are some regions where the fiber axis bends and in these areas the plane spacing appears at an angle to the fiber axis. This result shows that the material we have synthesized is different than the GNF materials used in other studies [17].

Isothermal flow microcalorimetry reveals the degree of interaction of the adsorbate (hydrogen) with the sorbent. This method is sensitive to both the total heat of adsorption ΔH_{ads}^{total} , and the mass storage capacity, x_{wt} , as shown in eq. 1.

$$Q/m = \frac{1}{M_{H_2}} \Delta H_{ads}^{total} x_{wt} \quad (1)$$

Rather than measuring isosteric heats of adsorption as a function of coverage, here ΔH_{ads}^{total} refers to the total heat released in going from the clean surface to the equilibrium coverage, per mole of hydrogen adsorbed. In essence, eq. 1 translates the heat of adsorption from an adsorbate basis to a sorbent basis. The point of this relationship is to show that the measured quantity (Q/m) will track changes in both the mass capacity and the heat of adsorption. Therefore, this technique should reveal differences among various carbon sorbents if such differences are significant.

Figures 4-7 show the calorimetry data for hydrogen adsorption on various carbon materials. All of the heat data are normalized to the initial mass of the sorbent. In these experiments mass change following adsorption is difficult to detect. Figure 4 shows the calorimetry data for BPL, a typical activated carbon used for natural gas storage [18]. The significance of the structure observed in the calorimetric curves is presently under investigation. Peak heights and areas in Figs. 4-7 are much smaller than those observed in typical chemisorption experiments [19].

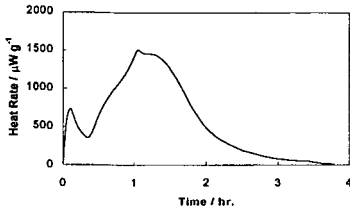


Figure 4: Hydrogen adsorption calorimetry data for BPL; hydrogen flow rate, 10 cc/min, 25 °C.

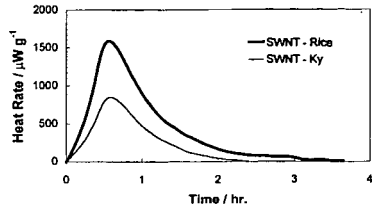


Figure 5: Hydrogen adsorption calorimetry data for carbon nanotubes; hydrogen flow rate, 10 cc/min, 25 °C.

Figure 5 shows the calorimetry data for hydrogen adsorption on the carbon nanotube samples. The Rice University sample displays a higher peak height and area than the University of Kentucky sample. This result can be rationalized either by a higher fraction of nanotubes or more active residual soot in the Rice sample. While the differences between these samples may be significant, as we will see later the total heat released is comparable to that when activated carbon is exposed to hydrogen (Fig. 4, Table 2).

One concern with the nanotube samples was whether hydrogen could access the interior of the tubes. If the tube interiors were not accessible, we might expect a lower measured heat due to a lower heat of adsorption on the tube exterior, as well as a lower mass capacity [6]. Figure 6 compares the hydrogen adsorption calorimetry for the Rice sample in both nanotube and “nanopipe” form. Processing the nanotubes to make pipes increases the degree of interaction of the hydrogen with the nanotube sample. While the effect of cutting the tubes is not extremely large, it is the most significant change observed in this study. Several possible explanations for this behavior exist. The processing step could: 1) increase surface area through opening the tube ends, 2) increase the heat of adsorption due to allowing access to more energetic surface sites, 3) increase adsorption capacity. We cannot rule out any of these possibilities at the present time. The initial rate of heat release is also significantly higher for the cut sample, which may indicate a different mechanism of adsorption or increased availability to sites with a higher adsorption potential.

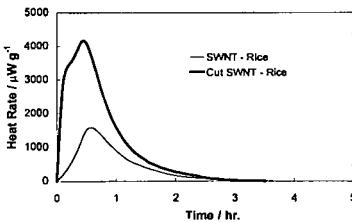


Figure 6: Hydrogen adsorption calorimetry data on carbon nanotubes; hydrogen flow rate, 10 cc/min, 25 °C.

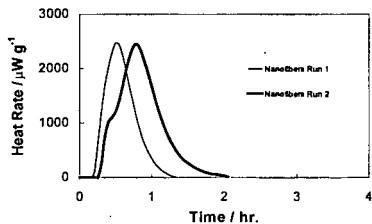


Figure 7: Hydrogen adsorption calorimetry data on synthetic carbon nanofibers; hydrogen flow rate, 10 cc/min, 25 °C.

Figure 7 shows the hydrogen adsorption calorimetry data for our nanofibers. This plot shows two different runs on the same sample. Following the first run the sample was placed in a vacuum oven at ~100 °C overnight and the experiment was repeated under identical conditions. The apparent shift in the peak maximum toward longer times is not significant because the zero on the time axis is arbitrary. Qualitatively the peak shape and height appear consistent from these two runs. The reasonable agreement between runs demonstrates the reproducibility of the technique.

The total heat released in the adsorption process (eq. 1) can be obtained simply by integrating the calorimetric signal over the period of the experiment. Table 2 shows the *semi-quantitative* results of these measurements. Since the statistical certainty on these measurements is not clear, we prefer to discuss these data qualitatively. The BPL sample shows one of the largest heat

releases obtained, consistent with the fact that this sample has a high micropore volume of 0.5 cm³/g making it a good sorbent for adsorbed natural gas storage [18]. The nanotube samples show somewhat decreased interaction with hydrogen relative to BPL. However, the "cut" nanotubes show the largest heat released of all samples, demonstrating either an increased heat of adsorption or an improved adsorption capacity. The nanofiber sample shows a total heat release that is somewhat less than that of BPL. The run-to-run variability can be judged qualitatively by comparing the two nanofiber runs. The results can be reproduced within about 27%. For the low-level signals observed in these experiments, we consider this degree of reproducibility very good.

Table 2: Semi-quantitative calorimetry results

Sample	Q/m (J/g)
BPL	7.8
U Ky Nanotubes	2.6
Rice University Nanotubes	5.5
"Cut" Rice University Nanotubes	13.9
Nanofibers, Run 1	4.3
Nanofibers, Run 2	5.9

The primary purpose of the calorimetry measurements was to look for extremely strong interactions between carbon nanotubes or nanofibers and hydrogen. The basis of comparison was a high quality activated carbon, BPL. From the measurements obtained we can say that the interactions of these materials are comparable to the interactions of activated carbon and hydrogen. Of course, the possibility exists for offsetting changes in the heat of adsorption and capacity (eq. 1), e.g. an increase in $\Delta H_{\text{ads}}^{\text{total}}$ and a decrease in x_{wt} . However, we interpret the data as suggesting a relative constancy of both quantities. Therefore, our initial question of some fundamentally different interactions between carbon nanotubes or nanofibers and hydrogen has been answered for conditions of atmospheric pressure and ambient temperature.

During the course of this experimental study, the computational chemistry community has been very active [6,20-25]. Several papers have sought to answer the same questions addressed here. These studies have made use of well-known interaction potentials for both C-H₂ and H₂-H₂ interactions. In one instance the carbon-hydrogen interaction potential (well depth) has been used as an adjustable parameter in an attempt to fit the experimental data of Rodriguez et. al. [3,4]. The conclusion from these studies is that the interaction potentials must be adjusted beyond physically reasonable limits in order to fit the data [21]. As a feasibility study, these computational studies are extremely valuable since years of materials optimization can be conducted in short order using adjustable computer models [6].

CONCLUSIONS

Hydrogen storage in new carbon nanostructures like carbon nanotubes and nanofibers appeared in the literature rather recently. Early experiments were conducted using different materials under different conditions leaving little conclusive evidence for good storage capacity. In this study we have characterized the interaction of hydrogen using isothermal flow microcalorimetry under constant conditions with high purity materials. Our data shows that the interaction of hydrogen with carbon nanotubes and nanofibers is comparable to the interaction of hydrogen with activated carbon. In view of our results, the results of attempts by other groups to reproduce the reported high storage capacities, and recent computational work, we conclude that carbon nanotubes and carbon nanofibers are not suitable as high-capacity hydrogen storage materials.

ACKNOWLEDGEMENTS

We acknowledge funding and permission to publish from Michael Winter and Jim Irish at UTRC. We enjoyed discussions of this work with Harvey Michels and Margaret Steinbugler of UTRC, Bryan Murach, Les Van Dine, and Tim Bekkedahl of International Fuel Cells, Sanjeev Mukerjee of Northeastern University, and Bob Bowman of the Jet Propulsion Laboratory.

REFERENCES

1. A.C. Dillon, K.M. Jones, T.A. Bekkedahl, C.H. Kiang, D.S. Bethune, and M. J. Heben, *Nature*, 386 (1997) 377.
2. M.A. DeLuchi, *Int. J. Hydrogen Energy*, 14 (1989) 81.
3. A. Chambers, C. Park, R.T.K. Baker, and N.M. Rodriguez, *J. Phys. Chem. B*, 102 (1998) 4253.

4. S. Hill, "Green Cars go Further with Graphite," *New Scientist*, December 28, 1996.
5. W. Liu and S.C. Fain, Jr., *Phys. Rev. B*, 47 (1993) 15965.
6. Q. Wang and J.K. Johnson, *J. Phys. Chem. B*, In press (1999).
7. C.C. Ahn, Y. Ye, B.V. Ratnakumar, C. Witham, R. C. Bowman, and B. Fultz, *Appl. Phys. Lett.*, 73 (1998) 3378.
8. Y. Ye et al., *Appl. Phys. Lett.* 74 (1999) 2307.
9. A.C. Dillon, T.A. Bekkedahl, A.F. Cahill, K.M. Jones, and M.J. Heben, In: *Proceedings of the 1995 DOE Hydrogen Program Review*, Vol. II, p. 521, NREL/CP-430-20036.
10. D. P. Valenzuela, and A. L. Myers, In: *Adsorption Equilibrium Data Handbook*, Prentice Hall, 1989.
11. T. Yildirim, Presented at the MRS Symposium, Boston MA, Paper S1.4, December 1998.
12. E. Brosha, Presented at the MRS Symposium, Boston MA, Paper S2.9, December 1998.
13. cnst.rice.edu/tubes/index.shtml
14. www.carbolex.com
15. A. Thess et. al., *Science*, 273 (1996) 483.
16. J. Liu et. al., *Science*, 280 (1998) 1253.
17. N.M. Rodriguez, *J. Mater. Res.*, 8 (1993) 3233.
18. J. Sun, S. Chen, M.J. Rood, and M. Rostam-Abadi, *Energy and Fuel* 12 (1998) 1071.
19. S. Satyapal, T. Filburn, J. Trela, J. Strange, "Novel Amine Sorbents for Separation of Carbon Dioxide", Submitted to: *Industrial and Engineering Chemistry Research*, 1998.
20. Q. Wang and J.K. Johnson, *J. Chem. Phys.*, 110 (1999) 577.
21. Q. Wang and J.K. Johnson, *J. Phys. Chem. B*, 103 (1999) 277.
22. Q.Y. Wang and J.K. Johnson, *Molecular Physics*, 95 (1998) 299.
23. Q.Y. Wang and J.K. Johnson, *Int. J. Thermophysics*, 19 (1998) 835-844.
24. F. Darkrim and D. Levesque, *J. Chem. Phys.*, 109 (1998) 4981.
25. M. Rzepka, P. Lamp, M.A. de la Casa-Lillo, *J. Phys. Chem. B*, 102 (1998) 10894.